Planta (2012) 236:1447–1458
DOI 10.1007/s00425-012-1695-x

ORIGINAL ARTICLE

Flavodoxin displays dose-dependent effects on photosynthesis and stress tolerance when expressed in transgenic tobacco plants

Romina D. Ceccoli · Nicolás E. Blanco · María E. Segretin · Michael Melzer · Guy T. Hanke · Renate Scheibe · Mohammad-Reza Hajirezaei · Fernando F. Bravo-Almonacid · Néstor Carrillo

Received: 26 April 2012 / Accepted: 16 June 2012 / Published online: 5 July 2012

Abstract Ferredoxins are iron–sulfur proteins involved in various one-electron transfer pathways. Ferredoxin levels decrease under adverse environmental conditions in photosynthetic organisms. In cyanobacteria, this decline is compensated by induction of flavodoxin, an isofunctional flavoprotein. Flavodoxin is not present in higher plants, but transgenic *Nicotiana tabacum* lines accumulating *Anabaena* flavodoxin in plastids display increased tolerance to different sources of environmental stress. As the degree of tolerance correlated with flavodoxin dosage in plastids of nuclear-transformed transgenic tobacco, we prepared plants expressing even higher levels of flavodoxin by direct plastid transformation. A suite of nuclear- and chloroplast-transformed lines expressing a wide range of flavodoxin levels, from 0.3 to 10.8 μmol m^{-2}, did not exhibit any detectable growth phenotype relative to the wild type. In the absence of stress, the contents of both chlorophyll *a* and carotenoids, as well as the photosynthetic performance (photosystem II maximum efficiency, photosystem II operating efficiency, electron transport rates and carbon assimilation rates), displayed a moderate increase with flavodoxin concentrations up to 1.3–2.6 μmol flavodoxin m^{-2}, and then declined to wild-type levels. Stress tolerance, as estimated by the damage inflicted on exposure to the pro-oxidant methyl viologen, also exhibited a bell-shaped response, with a significant, dose-dependent increase in tolerance followed by a drop in the high-expressing lines. The results indicate that optimal photosynthetic performance and stress tolerance were observed at flavodoxin levels comparable to those of endogenous ferredoxin. Further increases in flavodoxin content become detrimental to plant fitness.

Keywords Flavodoxin · Ferredoxin · Oxidative stress · Transgenic plants · Transplastomic transformation

Abbreviations

1-*qP*	Excitation pressure of PSII
A_{CO_2}	CO_2 assimilation rate
AL	Actinic light
ETR	Electron transport rate
F'_v/F'_m	Maximum efficiency of PSII
Fd	Ferredoxin
Fld	Flavodoxin

R. D. Ceccoli · N. E. Blanco · N. Carrillo (✉)
División Biología Molecular, Facultad de Ciencias Bioquímicas y Farmacéuticas, Instituto de Biología Molecular y Celular de Rosario (IBR, CONICET), Universidad Nacional de Rosario, Suipacha 531, S2002LRK Rosario, Argentina
e-mail: carrillo@ibr.gov.ar

Present Address:
N. E. Blanco
Department of Plant Physiology, Umeå Plant Science Centre, Umeå University, 901 87 Umeå, Sweden

M. E. Segretin · F. F. Bravo-Almonacid
Laboratorio de Virología y Biotecnología Vegetal, Instituto de Investigaciones en Ingeniería Genética y Biología Molecular (INGEBI, CONICET), C1428ADN Ciudad Autónoma de Buenos Aires, Argentina

M. Melzer · M.-R. Hajirezaei
Leibniz-Institut für Pflanzengenetik und Kulturpflanzenforschung, Corrensstrasse 3, 06466 Gatersleben, Germany

G. T. Hanke · R. Scheibe
Pflanzenphysiologie, FB Biologie/Chemie, Universität Osnabrück, 49069 Osnabrück, Germany

F. F. Bravo-Almonacid
Departamento de Ciencia y Tecnología, Universidad Nacional de Quilmes, Bernal, Buenos Aires, Argentina

FNR	Ferredoxin-NADP$^+$ reductase
F_v/F_m	Maximum quantum yield of PSII
GSH	Reduced glutathione
GSSG	Oxidized glutathione
MV	Methyl viologen
NIR	Near infrared
NPQ	Non-photochemical quenching
PETC	Photosynthetic electron transport chain
pfld	Transgenic tobacco lines expressing Fld from the nuclear genome
tfld	Transplastomic tobacco lines expressing Fld
PS	Photosystem
Q_A	Primary quinone acceptor of PSII
ROS	Reactive oxygen species
TEM	Transmission electron microscopy
WT	Wild-type
$\Delta P700_{max}$	Maximum P700 oxidation
Φ_{PSII}	Operating efficiency of PSII

Introduction

The ferredoxins (Fds) found in photosynthetic organisms are acidic 11-kDa proteins which contain a single [2Fe–2S] cluster. Fd operates as a mobile one-electron carrier at low redox potentials (Hanke et al. 2004; Hase et al. 2006). In chloroplasts and cyanobacteria, Fd is the final acceptor for the electrons generated by the oxidation of water to oxygen, which are conveyed through the photosynthetic electron transport chain (PETC). Fd is reduced by the light-dependent reaction of photosystem (PS) I and delivers reducing equivalents to several enzymes belonging to different metabolic, dissipative and regulatory pathways (Knaff 2005; Hase et al. 2006). In a reaction catalyzed by ferredoxin-NADP$^+$ reductase (FNR), reduced Fd is used as an electron donor to generate NADPH, which is required for the reducing steps in CO_2 assimilation and other biosynthetic routes (Carrillo and Ceccarelli 2003). Fd also provides reducing equivalents for nitrogen and sulfur assimilation (Hase et al. 2006), for the regulation of enzymatic activity via Fd-thioredoxin reductase (Scheibe 1991; Schürmann and Buchanan 2008), and for the regeneration of antioxidants such as ascorbate (Miyake and Asada 1994) and peroxiredoxin (Dietz et al. 2006). In addition, reduced Fd serves as an electron shuttle for cyclic electron flow, which enhances the proton gradient formation necessary to generate the ATP utilized for CO_2 assimilation, and helps to relieve the electron pressure on the PETC by induction of a thermal dissipative mechanism (NPQ) when the photosynthetic efficiency is low due to excess excitation energy (Shikanai 2007).

Fd accumulates above the tight stoichiometry of its redox partners in the PETC (PSI, FNR) in both plants (Böhme 1978) and algae (Inda and Peleato 2002), reflecting its many functions in plastid physiology. Fd levels are down-regulated by iron deficiency and environmental stress (Erdner et al. 1999; Mazouni et al. 2003; Singh et al. 2004; Zimmermann et al. 2004; Tognetti et al. 2006; Ceccoli et al. 2011).

In cyanobacteria and some algae, Fd decline is compensated by induced expression of flavodoxin (Fld), an isofunctional electron carrier of 19 kDa that contains flavin mononucleotide as the prosthetic group (Hagemann et al. 1999; Singh et al. 2004; Sancho 2006). Fld shuttles electrons from PSI to FNR (Sancho 2006) and in diazotrophic organisms contributes to nitrogen fixation (Saito et al. 2011). In non-photosynthetic bacteria, Fld may be involved in other biochemical pathways such as methionine and biotin synthesis, activation of pyruvate-formate lyase, ribonucleotide reductase and oxidation of pyruvate (Sancho 2006), as well as oxidative stress response (Krapp et al. 2002).

These flavoproteins are absent in plants, but cyanobacterial Fld has been shown to engage in electron transfer with several plant systems in vitro, including FNR, PSI and Fd-thioredoxin reductase (Scheller 1996; Nogués et al. 2004; Tognetti et al. 2006). Moreover, transgenic plants generated by nuclear genome transformation with a chloroplast-targeted Fld gene from *Anabaena* sp. PCC7119 exhibited enhanced tolerance to iron starvation and to several sources of stress, including water deficit, extreme temperatures, xenobiotics and pathogen-induced cell death (Tognetti et al. 2006, 2007; Zurbriggen et al. 2008, 2009). *Medicago truncatula* plants expressing a plastid-directed Fld failed to display enhanced tolerance to salt toxicity, but the presence of the flavoprotein did protect nodule nitrogen-fixing activity under NaCl stress (Coba de la Peña et al. 2010). In addition, Fld overexpression in rhizobia led to delayed nodule senescence and tolerance to cadmium toxicity in alfalfa, resulting from changes in the antioxidant metabolism of the nodules (Redondo et al. 2009; Shvaleva et al. 2010). Interestingly, *Arabidopsis* plants expressing Fld from *Synechocystis* sp. in chloroplasts exhibited increased biomass yield even in the absence of stress and improved photosynthetic efficiency under drought conditions (Mckersie et al. 2010).

The mechanism of tolerance has been studied in transgenic tobacco plants (*Nicotiana tabacum* cv. Petit Havana). Fld accumulation in chloroplasts of these lines resulted in restoration of productive routes of electron distribution and suppression of reactive oxygen species (ROS) buildup in leaves (Tognetti et al. 2006). The protective effect resulted from functional replacement of decreased Fd by Fld (Blanco et al. 2011) and correlated with the dose of plastid-borne Fld

(Tognetti et al. 2006, 2007; Zurbriggen et al. 2008). The accumulation of this flavoprotein in chloroplasts of transgenic plants obtained by nuclear transformation was apparently limited by plastid import efficiency (Tognetti et al. 2006). The aim of this research was to determine whether higher levels of tolerance could be attained by increasing Fld contents, or if Fld overaccumulation was detrimental to plant fitness. To achieve this goal, we prepared tobacco lines expressing Fld directly from the chloroplast genome, obtained by plastid transformation (Wirth et al. 2006). Analysis of a combination of nuclear- and chloroplast-transformed lines, expressing widely different amounts of Fld, indicated that photosynthetic performance and stress tolerance increased with the contents of the transgenic product to reach a plateau at levels similar to those of endogenous Fd concentrations (~3 μmol Fd m^{-2}). Higher Fld accumulation in the transplastomic lines led to a decline in both photosynthetic activity and stress tolerance, approaching the values observed with the non-transformed wild-type (WT) plants.

Materials and methods

Construction of transplastomic vector and transformation of tobacco

A DNA fragment encoding *Anabaena* sp. PCC7119 Fld (GI 239747) was obtained by PCR amplification using primers 5′-GCAGAGCTCTCCATATGTCAAAG-3′ and 5′-GGTG CAGGTCTAGATTTTAC-3′, containing *Nde*I and *Xba*I recognition sites, respectively. For chloroplast transformation, amplified DNA was digested and inserted into compatible sites of plasmid pBSWutr (Wirth et al. 2006), under the control of the plastidic *rnn* and *psbA* promoters, to produce pBSWutr-Fld (Blanco et al. 2011).

Tobacco plants were subjected to plastid transformation with pBSWutr-Fld by particle bombardment as previously described (Wirth et al. 2006). After three rounds of regeneration on selective medium containing 500 μg mL^{-1} spectinomycin, homoplasmic *tfld* plants were obtained. Non-segregating homozygous transgenic tobacco lines (*pfld12-4 and pfld5-8*, T_{10} generation) generated by nuclear genome transformation were also used. Their preparation and properties have been described elsewhere (Tognetti et al. 2006). Line *pfld5-4* was obtained by crossing *pfld5-8* with the wild type, and plants of the T_1 generation were used throughout the experiments.

Plant growth and characterization

Seeds were germinated on Murashige–Skoog agar plates supplemented with 2 % (w/v) sucrose and, in the case of transformants, 500 μg mL^{-1} spectinomycin (*tfld*) or 100 μg mL^{-1} kanamycin (*pfld*). After 3 weeks, seedlings were transferred to soil and grown at 200 μmol quanta m^{-2} s^{-1}, 25 °C and a 16-/8-h photoperiod (growth chamber conditions). Unless otherwise stated, experiments were performed using 8-week-old specimens grown in soil. To improve reproducibility and facilitate comparisons between lines, we always assayed, side-by-side, leaves and tissues of the same developmental stage (the same node) in WT and transformed plants. The presence of Fld and Fd in leaf extracts of the various lines was determined by SDS-PAGE and immunoblot analysis using specific antisera (Ceccoli et al. 2011). Levels of the electron carriers were estimated by comparison with pure standards (Blanco et al. 2011). For light and electron microscopy, 1-mm^2 sections of source leaves were prepared as described previously (Blanco et al. 2011). An FEI Tecnai G2 Sphera transmission electron microscope (FEI, http://www.fei.com) was used for ultrastructural analysis at 120 kV.

Determination of photosynthetic parameters

Chlorophyll fluorescence measurements were performed using a pulse-modulated PAM-101 fluorometer with integrated PAM-103 (Walz, Effeltrich, Germany). In steady-state experiments, attached leaves were pre-illuminated for 5 h at 200 or 600 μmol quanta m^{-2} s^{-1}. F_v and F_m were determined after dark adaptation of leaves for 30 min. Subsequently, leaves were exposed to 200 or 600 μmol quanta m^{-2} s^{-1} of actinic light (AL), and light-adapted values (F'_v, F'_m) were determined after 30 min of AL exposure. Photosynthetic parameters (F_v/F_m, F'_v/F'_m, Φ_{PSII}, 1-*qP* and NPQ) were calculated as described previously (Baker 2008). Induction/relaxation NPQ curves were determined using the program of the MINI-PAM 2000 fluorometer (Walz). Light induction measurements were performed on attached leaves pre-illuminated at 200 μmol quanta m^{-2} s^{-1} for at least 3 h and dark adapted for 30 min, by application of a saturating pulse to obtain the F_m values. After 30 s, NPQ induction was followed over 6 min at 200, 600 or 1,000 μmol quanta m^{-2} s^{-1} of AL, and saturating pulses were applied every 30 s to obtain F'_m values. The AL was subsequently turned off, and the dark relaxation process was monitored at various times (0.5, 1, 2, 4 and 9 min) using saturating pulses.

The PAM-101 fluorometer system (Walz) was used to determine the redox state of P700 in the second youngest attached leaves. Plants were dark adapted for 30 min prior to each measurement. P700 was oxidized by near infrared (NIR) light and the $\Delta P700_{max}$ values were calculated from the changes in absorption at 830 and 860 nm (Backhausen et al. 1998; Voss et al. 2008).

CO_2 assimilation rates (A_{CO_2}) were determined using an infrared gas analyzer LI-6400 (LI-COR, Lincoln, NE) at

two light intensities (250 and 1,500 μmol quanta m^{-2} s^{-1}) for 3 min.

Analytical determinations

Glutathione

Thiol-containing compounds were extracted from frozen tobacco leaves using 0.1 M HCl and the acidic extract was neutralized with 90 mM NaOH. To determine total glutathione (GSH + GSSG), disulfide bonds were reduced using dithiothreitol and thiol groups were subsequently labeled by monobromobimane to produce fluorescent derivatives. The amount of oxidized glutathione (GSSG) was determined after irreversibly blocking the reduced glutathione (GSH) present in the extract with *N*-ethylmaleimide and then repeating the thiol labeling procedure. The fluorescent derivatives were separated using an AccQ-Tag C18 reversed-phase column (Waters, Milford, MA) with 100 mM potassium acetate (pH 5.5):methanol (91:9, v/v) for 12 min, followed by pure methanol for 8 min at a flow rate of 1 mL min^{-1} on a Waters HPLC system (Anderson et al. 1999). They were detected by fluorescence with excitation at 380 nm and emission at 480 nm and quantified by comparison with derivatized standards. The redox state was calculated as the percentage of reduced glutathione present in the total glutathione pool.

Tocopherols

Tocopherols were extracted as previously described (Abbasi et al. 2007) by grinding and homogenizing 50 mg of frozen leaf material in 1 mL of pure methanol. After 30 min of incubation at 25 °C, samples were centrifuged at 16,000*g* for 3 min and the supernatants were transferred to new tubes. The amount of α-tocopherol was determined by resolving the methanol extracts on a Gemini C18 reversed-phase column (Phenomenex, Torrance, CA) with an isocratic acetonitrile:methanol (85:15, v/v) mobile phase for 10 min at a flow rate of 1 mL min^{-1} on a Waters HPLC system. Tocopherols were detected by fluorescence with excitation at 295 nm and emission at 332 nm, and quantified by comparison with standards (Sigma-Aldrich, St Louis, MO).

Photosynthetic pigments

The levels of photosynthetic pigments were determined spectrophotometrically after ethanol extraction of leaf discs (Lichtenthaler 1987).

Methyl viologen treatment

The attached second and third youngest fully developed leaves were dipped into 100 μM methyl viologen (MV), 0.1 % (v/v) Tween-20 for 30 s and incubated under growth chamber conditions for up to 24 h. For short-term experiments, leaf discs (12-mm diameter) were floated topside up in 1 mL of water or 10 μM MV, and illuminated at 600 μmol quanta m^{-2} s^{-1} for 3 h (ion leakage) or 5 h (total chlorophyll content), as described previously (Tognetti et al. 2006; Ceccoli et al. 2011).

Purification of *Anabaena* Fld from tobacco leaf extracts and activity determinations

Anabaena Fld was purified from tobacco leaves by acetone precipitation and ion-exchange chromatography, essentially as described by Buchanan and Arnon (1971). After the last chromatographic step, tobacco Fd was pulled down using specific IgG antibodies bound to Protein A-Sepharose (Sigma-Aldrich). The mixture was incubated for 2 h at 4 °C under continuous shaking. Samples were centrifuged and supernatants used to assess the purity of *Anabaena* Fld and for activity determinations. Cytochrome *c* reductase activity was measured at 25 °C by monitoring the absorbance increase at 550 nm using $\varepsilon_{550} = 19$ mM^{-1} cm^{-1} (Shin 1971).

Statistical analyses

Data were analyzed using one-way ANOVA and Tukey multiple range tests. When the normality and/or equal variance assumptions were not met, Kruskal–Wallis ANOVA by rank and Dunn's multiple range tests were used. Two-sample analyses were done using Student's *t* test. The significance refers to statistical significance at $P < 0.05$.

Results

Preparation of transgenic tobacco plants expressing different levels of a cyanobacterial Fld in chloroplasts

Tobacco plants accumulating a cyanobacterial Fld in chloroplasts have been previously generated by *Agrobacterium*-mediated leaf disc transformation (Tognetti et al. 2006). Several nuclear-transformed lines had been obtained, expressing different levels of Fld (*pfld* series) due to positional effects (Tognetti et al. 2006). Comparison with transgenic siblings in which Fld was targeted to the cytosol suggested that maximal Fld accumulation in chloroplasts was limited by plastid import efficiency (Tognetti et al. 2006).

To produce transgenic lines expressing higher amounts of Fld, we engineered tobacco plants by direct chloroplast transformation. The transgene was inserted by homologous

recombination at a single *locus* in the plastid genome (Fig. 1a, see "Materials and methods"). As expected, independent specimens from homoplasmic lines (*tfld*, for ***t***ransplastomic plants containing the ***fld*** gene) did not show position effects, yielding essentially the same leaf Fld contents (Fig. 1b, lanes 5, 6). These plants expressed ~11 μmol Fld m^{-2} of leaf tissue, about fourfold more than the *pfld5-8* line which accumulated the maximum Fld level by nuclear expression (Fig. 1b, lanes 4–6). In *pfld* plants, two immunoreactive bands were generally detected (Fig. 1b, lanes 2–4). The band displaying lower electrophoretic mobility corresponds to chloroplast-associated Fld precursor that has not been imported, as previously demonstrated (Tognetti et al. 2006).

To confirm that *Anabaena* Fld was expressed as an active holoprotein, the electron carrier was isolated from leaves of the transplastomic plants (Fig. 1c). Purified Fld was able to accept electrons from recombinant *Anabaena* FNR in the cytochrome *c* reductase assay with specific activities of 6.65 ± 0.04 μmol cytochrome *c* mg^{-1} FNR min^{-1} at 1 μM Fld, similar to those reported for *Anabaena* Fld (Carrillo and Ceccarelli 2003). The results indicate that the cyanobacterial Fld was able to functionally assemble the flavin mononucleotide when expressed in chloroplasts.

Photosynthetic performance of transgenic plants accumulating different Fld contents in plastids

To study in more detail the effect of Fld dosage on the phenotypes of these plants under normal or stress conditions, we selected transgenic tobacco lines accumulating 0.3 (*pfld12-4*), 1.3 (*pfld5-4*), 2.6 (*pfld5-8*) and 10.8 (*tfld11*) μmol Fld m^{-2} of leaf tissue (Fig. 1b; Table 1). The levels of tobacco Fd were not affected by accumulation of the cyanobacterial protein (Fig. 1b) and were about 3 μmol Fd m^{-2} in all lines (Table 1).

The transgenic plants did not show phenotypic differences relative to WT siblings with respect to growth, biomass accumulation and water content (Table 1). Previous observations indicated that cell and chloroplast ultrastructure of *pfld* leaves were similar to that of WT tobacco (Tognetti et al. 2006; Blanco et al. 2011). Light microscopy (LM) and transmission electron microscopy (TEM) were used to characterize leaf structure of transplastomic tobacco plants. Histological analysis under the light microscope showed that the organization of palisade and spongy parenchyma, as well as the distribution of chloroplasts on the anticlinal and the inner periclinal cell walls, did not differ significantly (Fig. 2a, b). However, the whole population of chloroplasts in *tfld11* plants appeared smaller and round shaped compared to the ellipsoidal chloroplasts of WT leaves (Fig. 2a, b). This was confirmed by ultrastructure analysis (Fig. 2c–f). Compared to the wild type,

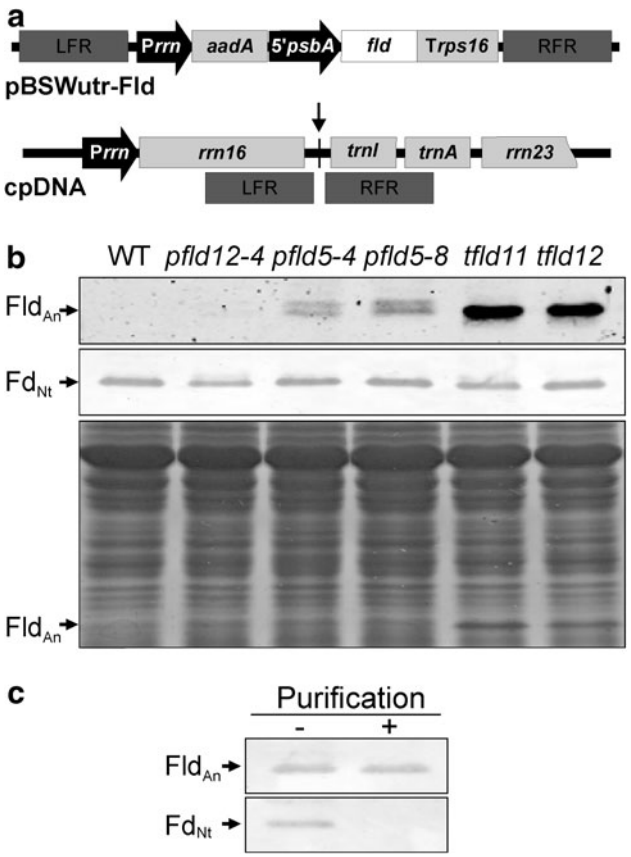

Fig. 1 *Anabaena* Fld expressed in chloroplasts of transgenic tobacco plants. **a** Schematic representation of the recombinant vector pBSWutr-Fld which contains the Fld coding region under the 5′-untranslated sequence and the promoter of the *psbA* gene (5′*psbA*). The transgenes are inserted by homologous recombination between *rrn16* and *trnI* plastid genes (*arrow*, cpDNA). The *aadA* sequence with a ribosome binding site is under the control of the P*rrn* promoter. LFR, left flanking region; RFR, right flanking region. **b** Fd and Fld levels in second fully expanded leaves of WT and Fld-expressing lines (*pfld* or *tfld*) were determined in leaf extracts from 8-week-old plants using SDS-PAGE and immunoblotting. Lanes *pfld* and *tfld* correspond to leaf extracts of transgenic plants generated by nuclear or plastid genome transformation, respectively. Cleared extracts equivalent to 2.8 mm^2 (Fld detection), 4.2 mm^2 (Fd detection) and 22.6 mm^2 (Coomassie Brilliant Blue staining) area of foliar tissue were loaded onto each lane. The electrophoretic mobilities of both electron carriers are indicated by *arrows*. The slower-migrating band reacting with Fld antiserum that could be visualized in some *pfld* lanes corresponds to unprocessed Fld precursor, as reported previously (Tognetti et al. 2006). Fld levels in *pfld12-4*, *pfld5-4*, *pfld5-8*, *tfld11* and *tfld12* were approximately 0.3, 1.3, 2.6, 10.8 and 10.7 μmol m^{-2}, respectively. Fd contents were about 3 μmol m^{-2} in all cases. **c** *Anabaena* Fld was purified from transplastomic tobacco (*tfld11*) leaf extracts as indicated in "Materials and methods". The presence of *Anabaena* (An) Fld and endogenous (Nt) Fd in crude (−) and purified (+) tobacco extracts was verified by SDS-PAGE and immunodetection assays using specific antibodies

the membrane network of chloroplasts of *tfld* plants was looser and less organized, and the grana were less stacked and distributed within the whole chloroplast area. The causes for this altered morphology and its relationship to

Table 1 Determination of physiological parameters and photosynthetic pigments in Fld-expressing and WT tobacco plants

	WT	*pfld12-4*	*pfld5-4*	*pfld5-8*	*tfld11*
Fd (μmol m^{-2})	3.2 ± 0.3^{a}	2.9 ± 0.2^{a}	3.2 ± 0.3^{a}	3.1 ± 0.3^{a}	3.0 ± 0.2^{a}
Fld (μmol m^{-2})	–	0.3 ± 0.0^{d}	1.3 ± 0.1^{c}	2.6 ± 0.2^{b}	10.8 ± 0.8^{a}
Number of nodes	8.33 ± 0.58^{a}	8.25 ± 0.50^{a}	8.40 ± 0.44^{a}	8.33 ± 0.82^{a}	8.00 ± 0.00^{a}
Height (cm)	40.50 ± 3.63^{a}	42.19 ± 2.26^{a}	39.83 ± 4.25^{a}	39.75 ± 5.40^{a}	40.67 ± 1.61^{a}
Internodal distance (cm)	3.68 ± 0.24^{a}	4.17 ± 0.21^{a}	3.90 ± 0.34^{a}	3.97 ± 0.75^{a}	4.07 ± 0.51^{a}
Aerial fresh weight (g)	50.24 ± 4.40^{a}	48.38 ± 6.22^{a}	46.28 ± 4.48^{a}	46.36 ± 6.04^{a}	50.24 ± 3.28^{a}
Aerial dry weight (g)	4.64 ± 0.72^{a}	4.23 ± 0.74^{a}	4.24 ± 0.77^{a}	4.28 ± 0.47^{a}	4.58 ± 0.25^{a}
% H_2O	91.26 ± 0.95^{a}	91.28 ± 0.93^{a}	90.90 ± 0.93^{a}	90.75 ± 1.26^{a}	90.88 ± 0.16^{a}
Chlorophyll *a* (μg cm^{-2})	28.59 ± 1.74^{bcd}	31.21 ± 4.15^{abc}	34.23 ± 2.83^{a}	33.06 ± 1.98^{ab}	28.12 ± 1.47^{cde}
Chlorophyll *b* (μg cm^{-2})	8.76 ± 0.32^{a}	9.16 ± 1.09^{a}	9.21 ± 0.76^{a}	8.56 ± 0.25^{a}	9.09 ± 0.42^{a}
Carotenoids (μg cm^{-2})	4.13 ± 0.54^{cd}	4.66 ± 0.76^{bcd}	5.70 ± 0.56^{a}	5.61 ± 0.35^{ab}	5.01 ± 0.25^{abc}
Chlorophyll *a* + *b* (μg cm^{-2})	37.35 ± 2.06^{bcd}	40.37 ± 5.24^{abc}	43.44 ± 3.58^{a}	41.62 ± 1.44^{ab}	37.21 ± 1.88^{bcd}
Chlorophyll *a*/*b*	3.26 ± 0.08^{abc}	3.40 ± 0.09^{abc}	3.72 ± 0.07^{ab}	3.86 ± 0.11^{a}	3.09 ± 0.04^{bc}

Plants were grown in soil for 8 weeks in a growth chamber under the conditions described in "Materials and methods". Procedures to determine pigments are also given there. The second and third fully expanded leaves were used for Fd, Fld and pigment determinations. Values reported are mean ± SD of seven individual plants

Fld accumulation remain unclear. However, the changes were moderate and affected neither growth (Table 1) nor photosynthetic performance (see below). Moreover, chloroplasts from stressed plants or from plants with significant modifications in photosynthetic electron transport display major ultrastructural perturbations (Palatnik et al. 2003; Ortigosa et al. 2010; Blanco et al. 2011).

Analysis of photosynthetic pigments in fully expanded leaves revealed that *pfld12-4*, *pfld5-4* and *pfld5-8* plants contained 9, 19 and 15 % higher chlorophyll *a* content relative to WT siblings, respectively (Table 1). Although moderate, the increases were statistically significant. By contrast, the *tfld11* line did not show deviations from WT in chlorophyll *a* levels (Table 1). Similar results were obtained for carotenoids (Table 1), whereas there were no significant differences in the amount of chlorophyll *b* between lines (Table 1). The higher chlorophyll *a* contents of *pfld* plants were reflected in the total chlorophyll levels and the chlorophyll *a*/*b* ratio (Table 1). It should be noted that the increase of leaf pigments in Fld-expressing plants has been reported previously, but not discussed (Tognetti et al. 2006, 2007).

At 250 μmol quanta m^{-2} s^{-1}, carbon assimilation rates (A_{CO_2}) were similar for WT and all transgenic lines (Fig. 2g). When the same experiment was carried out at the saturating intensity of 1,500 μmol quanta m^{-2} s^{-1}, A_{CO_2} increased with Fld contents up to ~22 % over the wild type in the *pfld5-4* line, but declined again to WT values in *tfld11* (Fig. 2b). It is worth noting that under saturating light conditions, A_{CO_2} displayed a good correlation with chlorophyll *a* contents.

To determine if the different doses of Fld in chloroplasts affected the functionality and redox state of the PETC, chlorophyll fluorescence measurements under steady-state conditions were carried out at two light intensities (200 and 600 μmol quanta m^{-2} s^{-1} of AL). Moderate increases in most photosynthetic parameters, including PSII maximum quantum yield (F_v/F_m), PSII maximum efficiency (F'_v/F'_m), PSII operating efficiency (Φ_{PSII}) and electron transport rate (ETR), were observed at both light intensities in *pfld* plants, correlating with Fld levels, but they were abolished in the *tfld11* line (Table 2). In multi-sample comparisons, as depicted in Table 2, WT and *tfld11* plants did not show statistically significant differences. However, when the two lines were individually compared (excluding *pfld* siblings), several chlorophyll fluorescence parameters (F_v/F_m, F'_v/F'_m, Φ_{PSII} and ETR) were lower in *tfld11* plants, with $P < 0.05$ (data not shown). On the other hand, the excitation pressure (1-*qP*) on the primary quinone acceptor (Q_A) of PSII and the non-photochemical quenching (NPQ) parameter did not differ significantly between lines (Table 2). The collected results suggest that utilization of energy generated at PSII to conduct linear electron flow was more efficiently used in plants expressing Fld levels equivalent to those of endogenous Fd.

When dark-adapted plants are exposed to light, they undergo a transient increase in NPQ, which reaches a maximum and subsequently declines due to photochemical quenching to reach steady-state values. NPQ buildup relies on two components with different characteristic kinetics: a rapid phase of NPQ induction that involves the generation of a ΔpH across thylakoid membranes through photosynthetic electron transport, followed by a slower phase dependent on zeaxanthin turnover, which is dependent on ΔpH (Joliot and Finazzi 2010). If the light is turned off

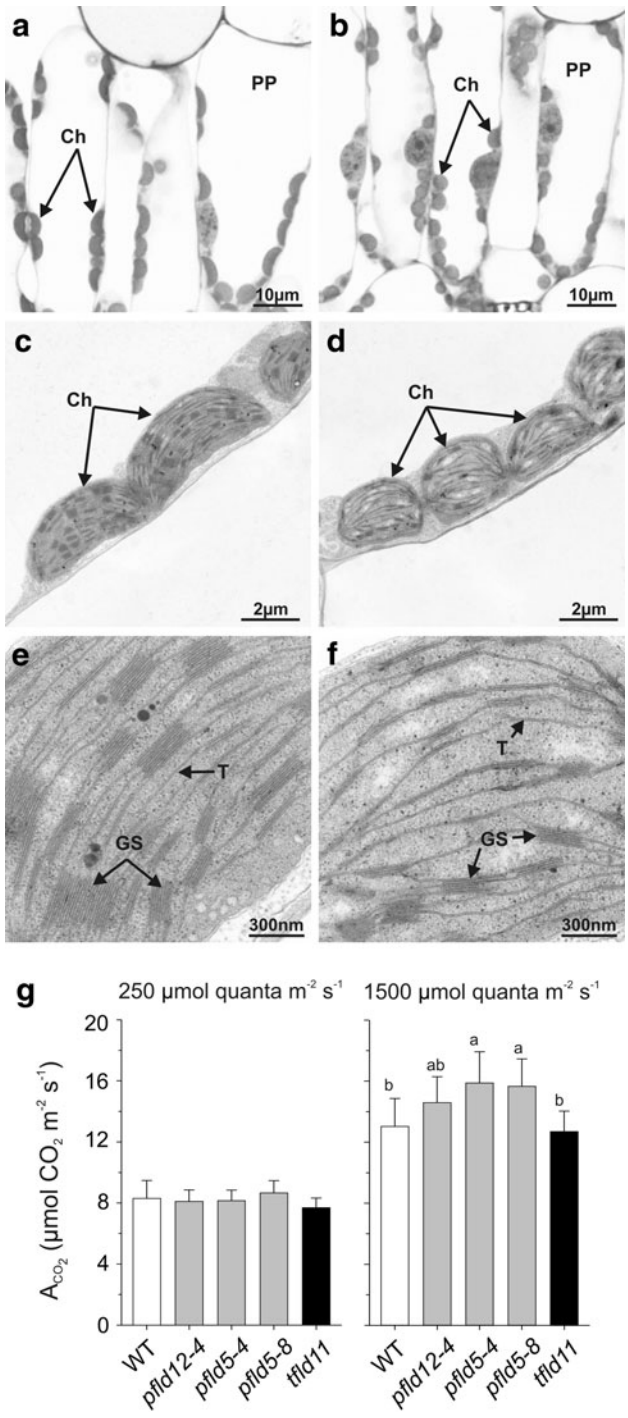

Fig. 2 Microscopic analysis of chloroplasts (**a**–**f**) and photosynthetic rates of WT and Fld-expressing tobacco leaves (**g**). Second fully expanded leaves were analyzed. Light microscopy of cross sections of leaves in WT (**a**) and *tfld* plants (**b**). Transmission electron micrographs of WT (**c**, **e**) and *tfld* chloroplasts (**d**, **f**). *Ch* chloroplast, *GS* grana stack, *PP* palisade parenchyma, *T* thylakoid. **g** Net CO_2 assimilation rates corresponding to 6-week-old WT, *pfld* and *tfld* plants at 250 or 1,500 μmol quanta m^{-2} s^{-1}. Values are mean ± SD of triplicate assays on three independent plants. Statistical differences among lines are indicated by *different letters* ($P < 0.05$)

when NPQ is at its maximum, NPQ relaxation proceeds through the same fast and slower components. Analysis of the time courses of both light induction and dark relaxation provides valuable data on the status of the PETC and the thermal dissipation of excess excitation energy at PSII (Blanco et al. 2011). Figure 3 shows induction/relaxation kinetics obtained for WT, *pfld* and *tfld* lines assayed under AL of 200, 600 or 1,000 μmol quanta m^{-2} s^{-1} after a dark adaptation period of 30 min. At 200 and 600 μmol quanta m^{-2} s^{-1}, all lines showed NPQ induction curves with a similar general shape (Fig. 3). The rapid ΔpH-dependent phase was completed in 1.2–2.5 min, with a maximum NPQ between 0.9 and 1.4, whereas at 1,000 μmol quanta m^{-2} s^{-1} NPQ did not entirely reach its saturation maximum during the 6-min time frame of AL exposure. Moreover, at this high light intensity, there were significant differences between the amplitudes of the various lines, with a moderate increase in the NPQ maximum as Fld contents were raised (Fig. 3). By contrast, relaxation time courses did not vary between lines (Fig. 3). The results suggest that the presence of Fld could improve the ability of the transformed plant to deploy an enhanced NPQ response.

PSI contains higher chlorophyll *a* levels than PSII (Fan et al. 2007). Chlorophyll *a* was moderately augmented in nuclear-transformed lines expressing Fld (Table 1, see also Tognetti et al. 2006, 2007), suggesting that these plants could be enriched in PSI. We evaluated this possibility by measuring P700 turnover in all lines. The redox status of P700 pigments ($\Delta P700_{max}$) in PSI was determined by monitoring the absorbance changes at 830 nm using NIR illumination to preferentially oxidize the PSI reaction center. In plants pre-illuminated at 600 μmol quanta m^{-2} s^{-1} for 5 h and dark adapted for 30 min, $\Delta P700_{max}$ increased with Fld contents to reach levels ~59 % over WT values in *pfld5-4*, but declined to a level below the wild type in *tfld11* plants (Table 2). Similar results were obtained when plants were pre-treated at 200 μmol quanta m^{-2} s^{-1}, although differences were less significant (Table 2). The increase in $\Delta P700_{max}$ suggests that when levels of Fld are similar to those of the endogenous Fd, there is higher efficiency in P700 oxidation and/or higher amounts of PSI reaction center available for oxidation.

Fld levels in chloroplasts affect the oxidative stress tolerance of tobacco plants

Previous results have shown that tobacco plants accumulating Fld in chloroplasts display enhanced tolerance to several sources of stress (Tognetti et al. 2006). We thus evaluated the effect of Fld dosage on stress tolerance by exposing tobacco leaves to MV, a redox-cycling herbicide

Table 2 Determination of chlorophyll fluorescence and P700 oxidation parameters in Fld-expressing and WT tobacco plants

	WT	*pfld12-4*	*pfld5-4*	*pfld5-8*	*tfld11*
200 µmol quanta m^{-2} s^{-1}					
F_v/F_m	0.726 ± 0.038^{ab}	0.735 ± 0.013^{ab}	0.755 ± 0.026^{a}	0.752 ± 0.014^{a}	0.677 ± 0.027^{b}
F'_v/F'_m	0.640 ± 0.038^{ab}	0.656 ± 0.011^{ab}	0.676 ± 0.013^{a}	0.674 ± 0.010^{a}	0.579 ± 0.022^{b}
Φ_{PSII}	0.603 ± 0.042^{ab}	0.629 ± 0.022^{ab}	0.649 ± 0.016^{a}	0.643 ± 0.023^{a}	0.526 ± 0.020^{b}
NPQ	0.251 ± 0.095^{b}	0.272 ± 0.065^{b}	0.297 ± 0.063^{b}	0.272 ± 0.089^{b}	0.199 ± 0.070^{b}
1-*qP*	0.058 ± 0.023^{b}	0.042 ± 0.028^{b}	0.040 ± 0.023^{b}	0.046 ± 0.025^{b}	0.091 ± 0.009^{b}
ETR	50.68 ± 3.52^{cd}	52.80 ± 1.83^{cd}	54.52 ± 1.32^{c}	54.01 ± 1.93^{c}	44.21 ± 1.68^{d}
$\Delta P700_{max}$	739 ± 122^{b}	875 ± 129^{ab}	991 ± 134^{a}	1025 ± 110^{a}	705 ± 83^{b}
600 µmol quanta m^{-2} s^{-1}					
F_v/F_m	0.673 ± 0.017^{cd}	0.652 ± 0.044^{cd}	0.711 ± 0.011^{c}	0.709 ± 0.013^{c}	0.563 ± 0.09^{d}
F'_v/F'_m	0.484 ± 0.040^{cd}	0.491 ± 0.031^{cd}	0.556 ± 0.024^{c}	0.554 ± 0.026^{c}	0.383 ± 0.014^{d}
Φ_{PSII}	0.417 ± 0.048^{cd}	0.416 ± 0.028^{cd}	0.493 ± 0.038^{c}	0.491 ± 0.035^{c}	0.320 ± 0.023^{d}
NPQ	0.504 ± 0.149^{a}	0.366 ± 0.051^{ab}	0.454 ± 0.052^{a}	0.454 ± 0.100^{a}	0.521 ± 0.155^{a}
1-*qP*	0.140 ± 0.030^{a}	0.152 ± 0.033^{a}	0.115 ± 0.033^{a}	0.115 ± 0.027^{a}	0.166 ± 0.040^{a}
ETR	105.19 ± 10.71^{ab}	104.80 ± 6.25^{ab}	124.16 ± 9.63^{a}	123.76 ± 8.83^{a}	80.58 ± 5.82^{b}
$\Delta P700_{max}$	661 ± 169^{bc}	946 ± 123^{ab}	1053 ± 228^{a}	1001 ± 216^{a}	529 ± 116^{c}

Eight-week-old plants were incubated for 5 h at 200 or 600 µmol quanta m^{-2} s^{-1}, and dark incubated for 30 min prior to dark-adapted measurements (F_v/F_m). Light-adapted determinations were performed after 30 min of exposure to 200 or 600 µmol quanta m^{-2} s^{-1}. NIR light was used to oxidize P700. All measurements were carried out on second and third fully expanded leaves. Data reported are mean ± SD of at least six measurements on independent plants

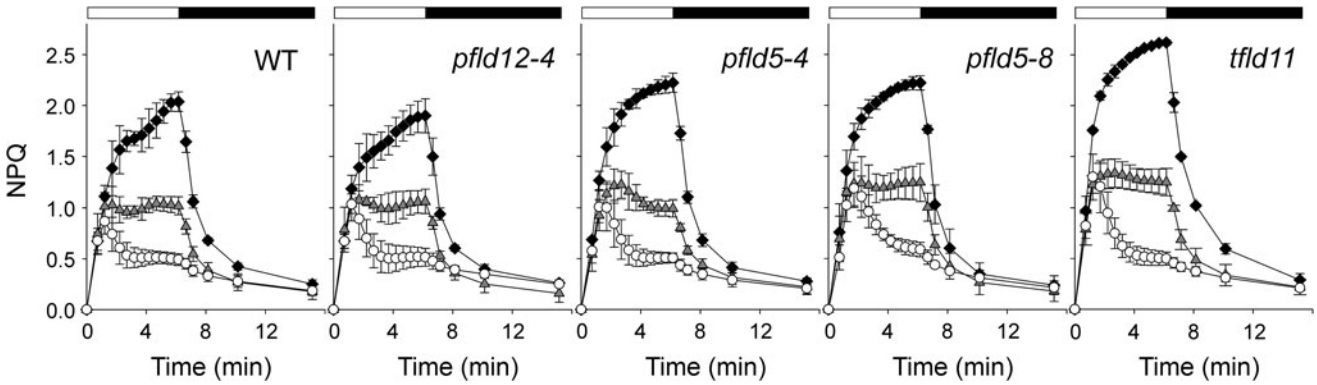

Fig. 3 Induction/relaxation curves of non-photochemical quenching in plants containing various amounts of Fld. NPQ measurements were carried out on second fully expanded leaves using induction (*white boxes*) and relaxation (*black boxes*) periods of 6 and 9 min, respectively. Plants were illuminated at 200 µmol quanta m^{-2} s^{-1} for at least 3 h, dark-adapted for 30 min and assayed at 200 (*white circles*), 600 (*gray triangles*) or 1,000 (*black diamonds*) µmol quanta m^{-2} s^{-1} of AL. Values are mean ± SD of three to four assays on independent plants

that propagates superoxide radicals by accepting electrons from PSI, one at a time, and transferring them to oxygen (Babbs et al. 1989). Typical symptoms exhibited by attached leaves of all lines treated with MV are illustrated in Fig. 4a. The number and severity of the chlorotic lesions were less significant when higher levels of Fld accumulated in the transgenic plants, reaching the maximum MV tolerance at 1.3–2.6 µmol Fld m^{-2} (Fig. 4a). Surprisingly, the extent of damage in *tfld11* leaves was similar to that observed in the *pfld12-4* line (Fig. 4a).

During short-term MV-exposure experiments using 12-mm diameter leaf discs, cell damage was estimated by measuring electrolyte leakage (Fig. 4b), and chlorophyll degradation (Fig. 4c). Protection from membrane deterioration by Fld expression was evident and dose dependent, although discs from *tfld11* plants were significantly less tolerant to MV toxicity than those obtained from *pfld5-4* and *pfld5-8* leaves (Fig. 4b). Five hours after MV treatment, total chlorophyll contents of WT discs declined by approximately 77 % with respect to discs of the same line

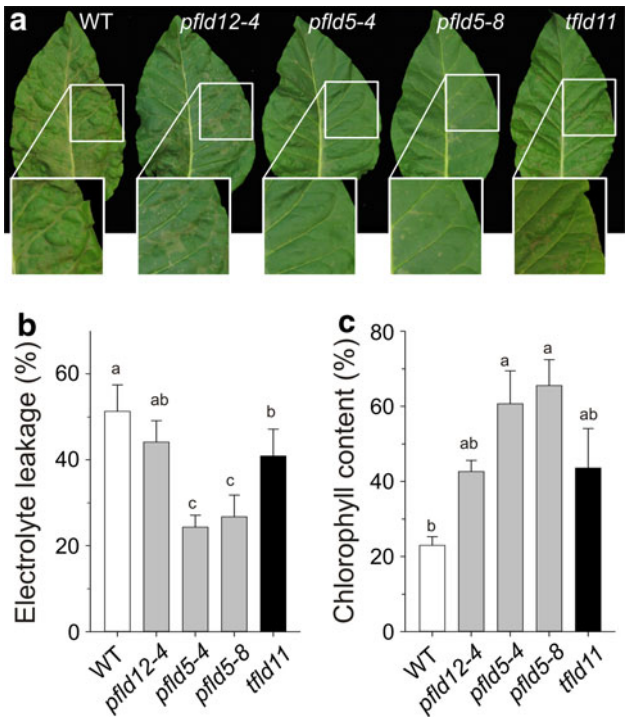

Fig. 4 Relationship between Fld levels expressed in chloroplasts and tolerance to MV toxicity. **a** The second youngest fully expanded leaves from 8-week-old WT and transgenic plants were exposed to MV as described in "Materials and methods". Pictures were taken 24 h after treatment. The Fld levels are given in Table 1. Electrolyte leakage (**b**) and total chlorophyll contents (**c**) were measured on leaf discs from WT and transformed plants after incubation with 10 μM MV for 3 h and 5 h, respectively, at 600 μmol quanta m^{-2} s^{-1}. The results are given as the percentages of ion leakage and total chlorophyll content relative to discs incubated in water under the same conditions. Values are mean ± SD of three assays. *Letters* above each bar represent the statistical significance of the observed differences among lines ($P < 0.05$): values with the same *letter* are not significantly different at $P < 0.05$ and those with different *letters* are significantly different at $P < 0.05$

incubated in the absence of MV. Photosynthetic pigment degradation was significantly lower in *pfld5-4* and *pfld5-8* discs, and only slightly lower in *pfld12-4* and *tfld11* tissue (Fig. 4c). Once again, tolerance of *tfld11* plants to MV toxicity was similar to that of *pfld12-4* discs (Fig. 4b, c), which contained ~30-fold less Fld.

The foliar tocopherol pool consists of more than 90 % α-tocopherol and has been proposed to participate in ROS detoxification together with hydrophilic antioxidants such as glutathione (Foyer and Noctor 2003). To further characterize Fld-expressing plants under oxidative stress conditions, α-tocopherol and glutathione levels were determined. The contents of α-tocopherol, total glutathione and the percentage of its reduced form (GSH) were similar in untreated leaves from all lines (Fig. 5). When plants were exposed to MV, α-tocopherol amounts increased in *pfld5-4* (71 %), *pfld5-8* (97 %) and *tfld11* (72 %) leaves, as compared to WT siblings (Fig. 5a). After MV treatment, a significant increase (~60 %) in the total glutathione content was observed in leaves, but there were no differences between lines (Fig. 5b). However, the degree of reduction within the glutathione pool did show significant differences, with a trend similar to that displayed by α-tocopherol contents in plants exposed to MV. The GSH fraction was highest in MV-treated *pfld5-4* (70 %) and *pfld5-8* (71 %) leaves, and lower (59 %) in *tfld11* leaves, relative to the wild type (Fig. 5c). As anticipated, antioxidant contents directly correlated with stress tolerance.

Discussion

Previous results have shown that the increased stress tolerance displayed by transgenic tobacco plants expressing a cyanobacterial Fld was dose dependent within the limits of Fld accumulation permitted by the nuclear transformation method employed (Tognetti et al. 2006, 2007). Those observations raised the possibility that (1) higher degrees of tolerance could be achieved by increasing Fld levels, although other scenarios can also be envisaged: (2) stress tolerance could saturate above a certain threshold of Fld content, or (3) Fld over-accumulation could become detrimental to plant welfare.

To probe these contrasting possibilities, we prepared transplastomic tobacco plants expressing *Anabaena* Fld from the chloroplast genome (Fig. 1a). As expected, all homoplasmic *tfld* lines accumulated the same level of Fld (Fig. 1b). Fld contents in *tfld* plants were ~fourfold higher than that of endogenous Fd (Fig. 1b). Fld was properly assembled and functional, and no significant growth phenotype was observed (Table 1), although Fld buildup did affect chloroplast ultrastructure in *tfld* plants (Fig. 2a–f). Endogenous Fd levels did not change in any of the transplastomic lines analyzed (Fig. 1b), indicating that Fd was not down-regulated by the higher amounts of final electron carriers in the PETC.

It is noteworthy that while chlorophyll *a* and carotenoid levels increased with Fld dose until 2.6 μmol Fld m^{-2}, beyond this threshold their contents became comparable to those of the wild type (Table 1). By contrast, there were no differences in chlorophyll *b* levels between lines (Table 1). Although moderate, pigment increases were consistently observed in hundreds of specimens, and *pfld5*-8 plants could be distinguished in the growth chamber from the wild type because their leaves look greener to the naked eye. The variable chlorophyll and carotenoid content phenotype might result from increased synthesis or lower turnover. It is not clear how Fld could contribute to these pathways. On the other hand, some ROS are produced even under normal growth conditions (Foyer and Noctor 2000)

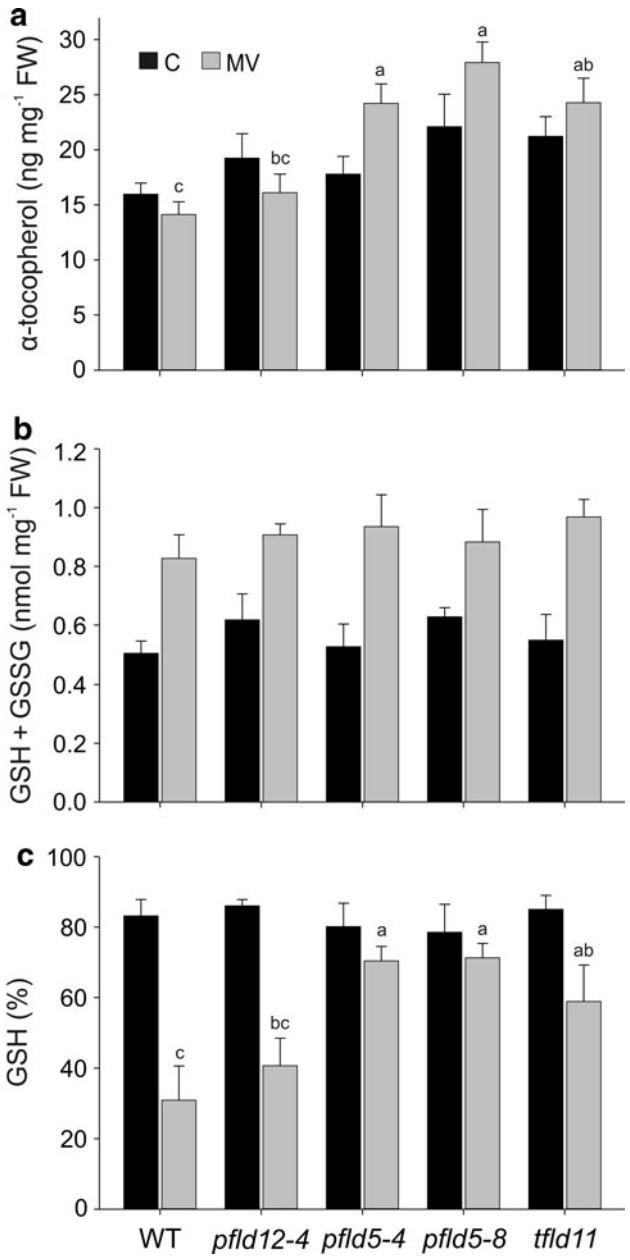

Fig. 5 Antioxidant levels in plants expressing different amounts of Fld. Contents of α-tocopherol (**a**) and total glutathione (GSH + GSSG) (**b**), and percentages of reduced glutathione (GSH) (**c**), were determined in MV-treated or control (C) tobacco leaves of different lines. The experimental procedures are described in "Materials and methods". Values are mean ± SD of four to six independent samples. *Letters* above each bar represent the statistical significance of the observed differences among lines ($P < 0.05$)

and this might lead to some chlorophyll degradation. The presence of Fld could alleviate this situation leading to higher steady-state chlorophyll levels. If so, the phenotype should be dependent on growth conditions, especially on the light intensity. Preliminary results (R. D. Ceccoli, unpublished observations) indicate that this is indeed the case.

Photosynthetic capacity and stress tolerance increased with Fld contents, with higher values obtained at 1.3–2.6 μmol Fld m^{-2}. Further Fld buildup in *tfld11* plants had detrimental consequences. The effects on the photochemical efficiency of both PSII and PSI (F_v/F_m, F'_v/F'_m, Φ_{PSII}, ETR and $\Delta P700_{max}$) were moderate, and in some cases they did not exhibit statistical significance (see superscripts in Tables 1, 2), although the trend was consistent in all cases. These differences translated into better CO_2 assimilation only when plants were assayed at high light intensity (Fig. 2g), and declined to WT levels at the highest Fld concentration (Tables 1, 2).

Previously, we have shown that Fld could engage in the dissipative response of the PETC via NPQ when Fd expression was silenced (Blanco et al. 2011). In the plants assayed in this study, with normal levels of endogenous Fd, the effect of Fld on NPQ induction was purely kinetic and only evident at high light intensities (Fig. 3). Deployment of NPQ relies primarily on electron transport through the PETC, both linear and cyclic. Our results suggest that under high electron pressure, Fld transiently increases electron flow in a dose-dependent manner, presumably by facilitating electron output at the terminal end of the PETC. Once steady-state was achieved after activation of the Calvin cycle, there were no significant differences between lines (Table 2), indicating that electron flow was limited by other factors. This relationship between PETC activity and Fld is intriguing and certainly deserves further research.

In contrast to photosynthetic activity, the Fld-dependent increase in stress tolerance and antioxidant capacity was always statistically significant, and although the *tfld11* plants with highest Fld accumulation performed worse than those with equivalent Fd and Fld concentrations, they remained more tolerant than the wild type (Figs. 4, 5). The levels of antioxidant metabolites increased in all lines as a response to MV challenge, but the fraction of the reduced forms was higher in plants expressing Fld (Fig. 5). The flavoprotein prevents ROS formation in chloroplasts (Tognetti et al. 2006; Zurbriggen et al. 2009), which leads to lower oxidation of glutathione and tocopherols and elevated steady-state contents of these antioxidants. The collected results indicate that the dose dependency of Fld effects follows a bell-shaped response.

The mechanism(s) underlying the negative effect of high Fld levels is unknown. The possibility that Fld accumulation becomes detrimental to photosynthesis due to the metabolic burden imposed by the need of synthesizing large amounts of the foreign protein seems highly unlikely, since *tfld11* plants do not display any growth phenotype (Table 1). Moreover, very high levels of transgenic proteins, up to 50 % of the total soluble proteins in mature leaves, have been expressed in chloroplasts using the transplastomic approach with no evident modification in

plant phenotype (Bally et al. 2009, 2011; Lentz et al. 2010). Recent observations indicate that synthesis of transplastomic proteins does occur at the expense of resident proteins, with Rubisco acting as a major nitrogen source (Bally et al. 2009, 2011). In contrast to those results, Fld is not a prominent soluble protein and Rubisco levels are not decreased in *tfld11* lines (Fig. 1b), indicating that amino acid availability does not represent a bottleneck that might explain the lower photosynthetic capacity and stress tolerance of these plants.

Flavin limitation due to the excess of the flavoprotein Fld can also be ruled out. An *Arabidopsis* mutant deficient in riboflavin synthesis displayed stunted growth, chlorosis and major inhibition of photosynthesis when cultivated at 140 μmol quanta m^{-2} s^{-1} (Ouyang et al. 2010), whereas *tfld11* plants were healthy and exhibited photosynthetic rates comparable to those of the wild type (Table 2).

It is possible that at the levels of expression obtained in *tfld11* plants (~fourfold over endogenous Fd), Fld could compete with the tobacco ferredoxins for reducing equivalents generated at the PETC and deliver them to stromal acceptors with lower efficiency. In vitro, *Anabaena* Fld has been shown to be less efficient than plant Fd in both $NADP^+$ and thioredoxin reduction (Nogués et al. 2004; Tognetti et al. 2006). Moreover, complementation by Fld of plants in which endogenous Fd had been knocked downed by RNA antisense or RNA interference approaches was only partial (Blanco et al. 2011), indicating that the cyanobacterial flavoprotein was indeed less efficient than Fd in vivo. Finally, it is also conceivable that an excess of electron acceptors at the reducing end of the PETC might introduce a perturbation in the chloroplast redox homeostasis that cannot be handled by the endogenous plastidic systems (Niyogi 2000; Scheibe 2004).

The expression of Fld in plants has provided a novel biotechnological tool to obtain badly needed stress-resistant crops (Zurbriggen et al. 2008; Coba de la Peña et al. 2010). Results presented in this article indicate that tolerance to environmental insults cannot be improved by increasing Fld levels above those obtained by nuclear transformation procedures. Optimal phenotypes are obtained at Fld levels comparable to those of endogenous Fd.

Acknowledgments This work was supported by grant PICT01-14648 from the Agencia Nacional de Promoción Científica y Tecnológica (ANPCyT), Argentina and by the Deutscher Akademischer Austauschdienst (DAAD), Germany. The authors wish to thank Dr. Anabella Lodeyro (IBR, CONICET, Argentina) for the generous gift of purified *Anabaena* FNR, and Mrs. Wally Wendt (IPK, Germany) for excellent technical assistance. NC, FFBA and MES are staff members and RDC is a fellow of CONICET, Argentina.

References

Abbasi AR, Hajirezaei M, Hofius D, Sonnewald U, Voll LM (2007) Specific roles of α- and γ-tocopherol in abiotic stress responses of transgenic tobacco. Plant Physiol 143:1720–1738

Anderson MT, Trudell JR, Voehringer DW, Tjioe IM, Herzenberg LA (1999) An improved monobromobimane assay for glutathione utilizing tris-(2-carboxyethyl) phosphine as the reductant. Anal Biochem 272:107–109

Babbs CF, Pham JA, Coolbaugh RC (1989) Lethal hydroxyl radical production in paraquat-treated plants. Plant Physiol 90:1267–1270

Backhausen JE, Emmerlich A, Holtgrefe S, Horton P, Nast G, Rogers JJM, Müller-Röber B, Scheibe R (1998) Transgenic potato plants with altered expression levels of chloroplast NADP-malate dehydrogenase: interactions between photosynthetic electron transport and malate metabolism in leaves and in isolated intact chloroplasts. Planta 207:105–114

Baker NR (2008) Chlorophyll fluorescence: a probe of photosynthesis in vivo. Annu Rev Plant Biol 59:89–113

Bally J, Nadai M, Vitel M, Rolland A, Dumain R, Dubald M (2009) Plant physiological adaptations to the massive foreign protein synthesis occurring in recombinant chloroplasts. Plant Physiol 150:1474–1481

Bally J, Job C, Belghazi M, Job D (2011) Metabolic adaptation in transplastomic plants massively accumulating recombinant proteins. PLoS One 6:e25289

Blanco NE, Ceccoli RD, Segretin ME, Poli HO, Voss I, Melzer M, Bravo-Almonacid FF, Scheibe R, Hajirezaei MR, Carrillo N (2011) Cyanobacterial flavodoxin complements ferredoxin deficiency in knocked-down transgenic tobacco plants. Plant J 65:922–935

Böhme H (1978) Quantitative determination of ferredoxin, ferredoxin-$NADP^+$ reductase and plastocyanin in spinach chloroplasts. Eur J Biochem 83:137–141

Buchanan BB, Arnon DI (1971) Ferredoxin from photosynthetic bacteria, algae, and higher plants. Methods Enzymol 23:413–440

Carrillo N, Ceccarelli EA (2003) Open questions in ferredoxin-$NADP^+$ reductase catalytic mechanism. Eur J Biochem 270:1900–1915

Ceccoli RD, Blanco NE, Medina M, Carrillo N (2011) Stress response of transgenic tobacco plants expressing a cyanobacterial ferredoxin in chloroplasts. Plant Mol Biol 76:535–544

Coba de la Peña T, Redondo FJ, Manrique E, Lucas MM, Pueyo JJ (2010) Nitrogen fixation persists under conditions of salt stress in transgenic *Medicago truncatula* plants expressing a cyanobacterial flavodoxin. Plant Biotechnol J 8:954–965

Dietz KJ, Jacob S, Oelze ML, Laxa M, Tognetti V, de Miranda SM, Baier M, Finkemeier I (2006) The function of peroxiredoxins in plant organelle redox metabolism. J Exp Bot 57:1697–1709

Erdner DL, Price NM, Doucette GJ, Peleato ML, Anderson DM (1999) Characterization of ferredoxin and flavodoxin as markers of iron limitation in marine phytoplankton. Mar Ecol Prog Ser 184:43–53

Fan DY, Hope AB, Smith PJ, Jia H, Pace RJ, Anderson JM, Chow WS (2007) The stoichiometry of the two photosystems in higher plants revisited. Biochim Biophys Acta 1767:1064–1072

Foyer CH, Noctor G (2000) Oxygen processing in photosynthesis: regulation and signaling. New Phytol 146:359–388

Foyer CH, Noctor G (2003) Redox sensing and signalling associated with reactive oxygen in chloroplasts, peroxisomes and mitochondria. Physiol Plant 119:355–364

Hagemann M, Jeanjean R, Fulda S, Havaux M, Joset F, Erdmann N (1999) Flavodoxin accumulation contributes to enhanced cyclic

electron flow around photosystem I in salt-stressed cells of *Synechocystis* sp. strain PCC6803. Physiol Plant 105:670–678

Hanke GT, Kimata-Ariga Y, Taniguchi I, Hase T (2004) A post genomic characterization of *Arabidopsis* ferredoxins. Plant Physiol 134:255–264

Hase T, Schürmann P, Knaff D (2006) The interaction of ferredoxin with ferredoxin-dependent enzymes. In: Golbeck JH (ed) Photosystem I: the light-driven plastocyanin:ferredoxin oxidoreductase. Advances in photosynthesis and respiration, vol 24. Springer, Dordrecht, pp 477–498

Inda LD, Peleato ML (2002) Immunoquantification of flavodoxin and ferredoxin from *Scenedesmus vacuolatus* (Chlorophyta) as iron-stress molecular markers. Eur J Phycol 37:579–586

Joliot PA, Finazzi G (2010) Proton equilibration in the chloroplast modulates multiphasic kinetics of nonphotochemical quenching of fluorescence in plants. Proc Natl Acad Sci USA 107:12728–12733

Knaff DB (2005) Ferredoxin and ferredoxin-dependent enzymes. In: Ort DR, Yocum CF (eds) Oxygenic photosynthesis: the light reactions. Kluwer Academic Publishers, Dordrecht, pp 333–361

Krapp AR, Rodriguez RE, Poli HO, Paladini DH, Palatnik JF, Carrillo N (2002) The flavoenzyme ferredoxin (flavodoxin)-NADP(H) reductase modulates NADP(H) homeostasis during the *soxRS* response of *Escherichia coli*. J Bacteriol 184:1474–1480

Lentz EM, Segretin ME, Morgenfeld MM, Wirth SA, Dus Santos MJ, Mozgovoj MV, Wigdorovitz A, Bravo-Almonacid FF (2010) High expression level of a foot and mouth disease virus epitope in tobacco transplastomic plants. Planta 231:387–395

Lichtenthaler HK (1987) Chlorophylls and carotenoids—pigments of photosynthetic biomembranes. Methods Enzymol 148:350–382

Mazouni K, Domain F, Chauvat F, Cassier-Chauvat C (2003) Expression and regulation of the crucial plant-like ferredoxin of cyanobacteria. Mol Microbiol 49:1019–1029

Mckersie BD, Bruce W, BASF Plant Science GMBH (2010) Transgenic plants with increased yield. USA patent WO2010/034652A1

Miyake C, Asada K (1994) Ferredoxin-dependent photoreduction of the monodehydroascorbate radical in spinach thylakoids. Plant Cell Physiol 35:539–549

Niyogi KK (2000) Safety valves for photosynthesis. Curr Opin Plant Biol 3:455–460

Nogués I, Tejero J, Hurley JK, Paladini D, Frago S, Tollin G, Mayhew SG, Gómez-Moreno C, Ceccarelli EA, Carrillo N, Medina M (2004) Role of the C-terminal tyrosine of ferredoxin-nicotinamide adenine dinucleotide phosphate reductase in the electron transfer processes with its protein partners ferredoxin and flavodoxin. Biochemistry 43:6127–6137

Ortigosa SM, Díaz-Vivancos P, Clemente-Moreno MJ, Pintó-Marijuan M, Fleck I, Veramendi J, Santos M, Hernández JA, Torne JM (2010) Oxidative stress induced in tobacco leaves by chloroplast over-expression of maize plastidial transglutaminase. Planta 232:593–605

Ouyang M, Ma J, Zou M, Guo J, Wang L, Lu C, Zhang L (2010) The photosensitive *phs1* mutant is impaired in the riboflavin biogenesis pathway. J Plant Physiol 167:1466–1476

Palatnik JF, Tognetti VB, Poli HO, Rodríguez RE, Blanco N, Gattuso M, Hajirezaei MR, Sonnewald U, Valle EM, Carrillo N (2003) Transgenic tobacco plants expressing antisense ferredoxin-NADP(H) reductase transcripts display increased susceptibility to photo-oxidative damage. Plant J 35:332–341

Redondo FJ, Coba de la Peña T, Morcillo CN, Lucas MM, Pueyo JJ (2009) Overexpression of flavodoxin in bacteroids induces changes in antioxidant metabolism leading to delayed senescence and starch accumulation in alfalfa root nodules. Plant Physiol 149:1166–1178

Saito MA, Bertranda EM, Dutkiewicz S, Bulygina VV, Morana DM, Monteiro FM, Follows MJ, Valois FW, Waterbury JB (2011) Iron conservation by reduction of metalloenzyme inventories in the marine diazotroph *Crocosphaera watsonii*. Proc Natl Acad Sci USA 108:2184–2189

Sancho J (2006) Flavodoxins: sequence, folding, binding, function and beyond. Cell Mol Life Sci 63:855–864

Scheibe R (1991) Redox-modulation of chloroplast enzymes: a common principle for individual control. Plant Physiol 96:1–3

Scheibe R (2004) Malate valves to balance cellular energy supply. Physiol Plant 120:21–26

Scheller HV (1996) In vitro cyclic electron transport in barley thylakoids follows two independent pathways. Plant Physiol 110:187–194

Schürmann P, Buchanan BB (2008) The ferredoxin/thioredoxin system of oxygenic photosynthesis. Antioxid Redox Signal 10:1235–1274

Shikanai T (2007) Cyclic electron transport around photosystem I: genetic approaches. Annu Rev Plant Biol 58:199–217

Shin M (1971) Ferredoxin-$NADP^+$ reductase from spinach. Methods Enzymol 23:440–447

Shvaleva A, Coba de la Peña T, Rincón A, Morcillo CN, García de la Torre VS, Lucas MM, Pueyo JJ (2010) Flavodoxin overexpression reduces cadmium-induced damage in alfalfa root nodules. Plant Soil 326:109–121

Singh AK, Li H, Sherman LA (2004) Microarray analysis and redox control of gene expression in the cyanobacterium *Synechocystis* sp. PCC 6803. Physiol Plant 120:27–35

Tognetti VB, Palatnik JF, Fillat MF, Melzer M, Hajirezaei MR, Valle EM, Carrillo N (2006) Functional replacement of ferredoxin by a cyanobacterial flavodoxin in tobacco confers broad-range stress tolerance. Plant Cell 18:2035–2050

Tognetti VB, Zurbriggen MD, Morandi EN, Fillat MF, Valle EM, Hajirezaei MR, Carrillo N (2007) Enhanced plant tolerance to iron starvation by functional substitution of chloroplast ferredoxin with a bacterial flavodoxin. Proc Natl Acad Sci USA 104:11495–11500

Voss I, Koelmann M, Wojtera J, Holtgrefe S, Kitzmann C, Backhausen JE, Scheibe R (2008) Knockout of major leaf ferredoxin reveals new redox-regulatory adaptations in *Arabidopsis thaliana*. Physiol Plant 133:584–598

Wirth S, Segretin ME, Mentaberry A, Bravo-Almonacid F (2006) Accumulation of hEGF and hEGF-fusion proteins in chloroplast-transformed tobacco plants is higher in the dark than in the light. J Biotechnol 125:159–172

Zimmermann P, Hirsch-Hoffmann M, Hennig L, Gruissem W (2004) GENEVESTIGATOR. *Arabidopsis* microarray database and analysis toolbox. Plant Physiol 136:2621–2632

Zurbriggen MD, Tognetti VB, Fillat MF, Hajirezaei MR, Valle EM, Carrillo N (2008) Combating stress with flavodoxin: a promising route for crop improvement. Trends Biotechnol 26:531–537

Zurbriggen MD, Carrillo N, Tognetti VB, Melzer M, Peisker M, Hause B, Hajirezaei MR (2009) Chloroplast-generated reactive oxygen species play a major role in localized cell death during the non-host interaction between tobacco and *Xanthomonas campestris* pv. *vesicatoria*. Plant J 60:962–973